

# The Properties of Optical Radiation Detectors and Radiometers



# The Properties of Optical Radiation Detectors and Radiometers

By

George P. Eppeldauer

**Cambridge  
Scholars  
Publishing**



The Properties of Optical Radiation Detectors and Radiometers

By George P. Eppeldauer

This book first published 2020

Cambridge Scholars Publishing

Lady Stephenson Library, Newcastle upon Tyne, NE6 2PA, UK

British Library Cataloguing in Publication Data

A catalogue record for this book is available from the British Library

Copyright © 2020 by George P. Eppeldauer

All rights for this book reserved. No part of this book may be reproduced, stored in a retrieval system, or transmitted, in any form or by any means, electronic, mechanical, photocopying, recording or otherwise, without the prior permission of the copyright owner.

ISBN (10): 1-5275-5590-9

ISBN (13): 978-1-5275-5590-7

# TABLE OF CONTENTS

Preface .....	viii
1. Introduction .....	1
2. Photodiodes .....	2
2.1. Radiometric characteristics of photodiodes .....	2
2.1.1. Quantum efficiency and spectral responsivity .....	3
2.1.2. Spatial responsivity .....	16
2.1.3. Angular responsivity and polarization dependence .....	30
2.1.4. Temperature dependent responsivity .....	34
2.1.5. Noise equivalent power (NEP) and detectivity ( $D^*$ ) .....	38
2.1.6. Radiometric sensitivity .....	41
2.1.7. Responsivity-linearity .....	42
2.2. Electronic characteristics of photodiodes .....	45
2.2.1. Shunt resistance .....	45
2.2.2. Noise .....	51
2.2.3. Drift .....	61
2.2.4. Settling time .....	63
2.2.5. Silicon photodiodes stability .....	64
3. Photoconductors .....	68
3.1. Photoconductive (PC) detector signal measurements .....	68
3.1.1. Current mode measurement .....	68
3.1.2. Voltage mode measurements .....	69
3.2. PC HgCdTe (MCT) detectors .....	72
4. Optical bolometers .....	74
4.1. Electrical operation .....	75
4.2. Thermal operation .....	76
4.3. Bolometer characteristics .....	79
4.3.1. Resistance .....	79
4.3.2. Linearity .....	79
4.3.3. Spatial responsivity .....	80
4.3.4. Upper roll-off frequency .....	81
4.3.5. Cool-down time and stability .....	83
4.3.6. Spectral responsivity .....	83
4.4. Electrical substitution bolometer .....	87

5. Pyroelectric detectors .....	92
5.1. Thermal characteristics .....	92
5.1.1. Temperature coefficient of responsivity .....	93
5.2. Electrical characteristics .....	96
5.2.1. Extension of upper roll-off frequency .....	101
5.2.2. Noise-equivalent current .....	104
5.3. Radiometric characteristics .....	105
5.3.1. Spectral reflectance of black coatings.....	105
5.3.2. Spectral responsivity .....	111
5.3.3. Spatial uniformity of responsivity.....	115
5.3.4. Linearity .....	120
5.3.5. Decrease of NEP.....	120
6. Thermopiles .....	129
7. Photomultiplier tubes (PMT).....	132
7.1. DC and AC measurement modes .....	133
7.2. PMT comparison to Si photodiode .....	134
8. Cryogenic thermal radiometers .....	136
8.1. Cryogenic thermal sensors (thermometers).....	137
8.1.1. Germanium and carbon resistance thermometers....	138
8.1.2. Rhodium-iron resistance thermometers .....	140
8.1.3. Cernox thin-film resistance thermometers .....	140
8.1.4. Si resistance thermometers .....	140
8.1.5. Superconducting kinetic inductance thermometer ...	141
8.1.6. High $T_c$ superconducting resistance (transition edge) thermometer .....	142
8.2. Cryogenic thermal sensor applications .....	143
8.2.1. Constant current biasing circuit for thermal sensors...	143
8.2.2. Bridge circuits .....	145
8.2.3. Sensitive cryogenic voltage amplifiers .....	151
8.2.4. Sensitivity comparison of temperature measuring circuits .....	155
8.2.5. Power measurements with thermal sensors .....	157
8.3. Temperature regulation and control for cryogenic thermal radiometers.....	161
8.4. Cryogenic Dewars .....	165
8.5. Cryogenic extrinsic (doped) infrared (IR) detectors .....	166
8.6. Cryogenic transimpedance amplifiers for doped IR detectors .....	169

9. Non-linearity issues .....	172
9.1. Definitions .....	172
9.2. Non-linearity caused by biasing and measuring circuits ...	176
9.3. Non-linearity of special devices .....	179
9.3.1. Detector arrays (cameras, spectrographs).....	179
9.3.2. Avalanche photodiodes .....	181
9.4. Non-linearity test methods.....	182
9.4.1. Recognized methods for assessing non-linearity ....	182
9.4.2. Other test methods.....	190
9.4.3. Uncertainty of non-linearity test methods.....	191
10. Comparison of detector characteristics .....	192
10.1. Selection of detectors for different applications .....	193
10.2. Electronic selection criteria of photodiodes .....	194
11. References .....	195
12. Problems.....	202
13. Solution of problems.....	203

# PREFACE

Improved detector technology in the past two decades opened a new era in the field of optical radiation measurements. An increased number of calibration and measurement facilities and procedures could be developed with lower measurement uncertainties using the newly developed detector/radiometer standards instead of traditionally applied source standards (blackbodies and lamps). Shrinking of the traditional source-based calibrations and the large increase of optical detector-based calibrations motivated the writing of this book series.

The book series is a comprehensive description of optical detector based radiometric practices. Instead of giving the traditional lexical-type tutorial information, a research-based material is systematically organized and described. The large number of examples cover modern detector applications in the field of radiometry, photometry, colorimetry, and radiation temperature measurements. All the discussed devices and applications have been implemented, realized, tested, verified, and evaluated. These applications are described to obtain uniform results with low measurement uncertainties. They are described with enough details to successfully repeat them by the readers/users. The applications and evaluations follow the recommendations of international standardization. The described subjects are detailed and distributed in five volumes.

Properties of radiometric quality detectors, their use and selection for optical radiometers, design considerations of radiometers and detector-based standards, description of spectral and broadband detector-based calibrations and measurements using modern setups based on the new radiometer standards are described for practicing scientists, engineers, and technicians.

The book series includes many hundreds of designs, drawings, measurement schemes, a large number of detector-based measurement and calibration setups, measurement equations and results, calibration-transfer and measurement methods/procedures all tested in practical applications.

In addition to reference level detector/radiometer calibrations, measurement of radiometric quantities used in practice (secondary laboratory and field applications), are discussed. Such quantities are radiant power, irradiance, and radiance. Measurement of spectral and broadband (integrated) quantities are discussed from 200 nm in the ultraviolet to 30  $\mu\text{m}$  in the infrared.

All discussed calibrations and measurements are traceable to the System International (SI) units through National Measurement Institutes (NMI) and/or the discussed intrinsic detector standards.

Linear and traceable measurement of detector output signals, including DC and AC photocurrent (sub-scale) and voltage measurements, detector-amplifier gain-calibrations, and gain-linearity tests are discussed in detail.

Uncertainty determination/calculation methods of detector-based measurements are described. It is a general rule for the discussed large number of design and application examples, to keep the calibration/measurement uncertainties low.

The author thanks all the colleagues listed in the references at the end of each volume for their help and contribution to perform the discussed large number of measurements and evaluations.

Dr. George P Eppeldauer, author



# 1. INTRODUCTION

Improved optical-detector technology in the past two decades opened a new era in the field of optical radiation measurements. Lower calibration and measurement uncertainties can be achieved with modern detector/radiometer (detector-based) standards than traditionally used source standards (blackbodies and lamps). The achievable lower uncertainties make it possible to decrease the gap between the 0.02 % (coverage factor  $k=2$ ) relative expanded uncertainty of cryogenic radiometer (primary standard) measurements and the two to three orders of magnitude higher uncertainties of field-level (source-based) optical radiation measurements.

The properties of radiometric (standards) quality detectors are to be known to use them as transfer or working standards and to perform radiometric, photometric and colour measurements with low uncertainties and with good long-term stabilities. The standards can propagate detector responsivity from reference calibration facilities to different radiometric applications. In order to obtain the lowest relative uncertainties associated with the spectral responsivity values, selection of detectors is an important task. Only single-element detectors are discussed here that can be calibrated for spectral power, irradiance, or radiance responsivity. The main requirement from these detectors/radiometers is that they should not increase the responsivity-uncertainty during a calibration transfer and a long-term use. In order to achieve this requirement between 200 nm and 30  $\mu\text{m}$ , the properties of several different types of optical detectors are discussed here.

## 2. PHOTODIODES

Photodiodes are the most frequently applied optical radiation detectors. The optical detector is a device in which incident optical radiation produces a measurable physical effect. The incident radiation is the input signal that produces an electrical output signal (current) that can be measured at the output of the detector. Photodiodes are widely used for radiometric scale transfer. They are the work horses of routine spectral responsivity measurements. They are also the fundamental building blocks of optical radiometers that can measure different radiometric quantities such as radiant (optical) power, irradiance, or radiance. Photodiodes are quantum detectors, they detect photons. They are mostly operated in photovoltaic measurement mode when biasing voltage or current is not applied to them. In order to obtain the lowest measurement uncertainties in calibrations and applications, selection of photodiodes is an important task. To help this task, the basic radiometric and electronic characteristics of photodiodes are discussed below.

### **2.1 Radiometric characteristics of photodiodes**

Photodiodes can be used to convert the input radiometric quantity into an output electrical quantity with high efficiency. The input optics mounted in front of a detector can help to convert the input radiometric quantity into radiant power which is measured by the detector itself. The input power (carried with photons) is then converted into electrons that can be measured as detector output current. In radiant power measurement mode, the input power incident on the detector, under-fills the active area of the detector and the total power in the incident beam is measured. In irradiance and radiance measurement modes the detector or an aperture in front of the detector is overfilled by the incident radiation. However, the detector is under-filled when the input aperture is used. Consequently, in all three radiometric measurement modes, the detector itself will always measure radiant power.

The detector should have a spatially uniform response if the incident beam is smaller than the detector active area to receive the same

responsivity at different beam positions. The responsivity is equal to the output quantity divided by the input quantity. Good spatial uniformity of responsivity may be required when the incident-beam can hit the detector at different positions or non-uniform input radiation is measured.

The responsivity is one of the most important characteristics of a radiometric (standards) quality detector. The responsivity is a wavelength dependent function. The shape and the wavelength coverage of this function dominantly determine the application area for a detector. The spectral responsivity is utilized to transfer detector calibration from a calibration laboratory to different field applications. Therefore, the responsivity changes should be known to evaluate the uncertainty of a responsivity measurement or a responsivity transfer.

There are other important responsivity-related detector characteristics. Linearity shows if the responsivity is proportional to the incident power on the detector. Also, the responsivity can be a function of the angle of the incident beam (relative to the normal of the detector front surface) and the temperature of the detector. The radiometric sensitivity of a detector also should be known to determine the dynamic range of radiometric power measurements.

### **2.1.1. Quantum efficiency and spectral responsivity**

The internal quantum efficiency (IQE) of a detector is the ratio of the number of generated electron-hole pairs to the number of incident and absorbed photons:

$$\text{IQE} = \frac{\text{electrons}}{\text{photons}} \quad (1)$$

The IQE shows how efficient the responsivity of a detector is. The responsivity is equal to a ratio where the output signal is divided by the input signal. For example, silicon detectors with multiple input reflections have been worked out to minimize reflection loss. The reflection loss can be a few times ten percent for different photodiodes. Silicon photodiodes with IQE close to 100 % are used in light-trapping detectors. Figure 1 shows the measurement results

obtained on a Hamamatsu 1337<sup>1</sup> silicon trap-detector where the outputs of six photodiodes are connected parallel (electrically) in a tunnel-shape arrangement [1]. Most of the incident radiation is absorbed by the photodiodes after six reflections. The output (exiting) radiation divided by the incident radiation is equal to the transmittance of this trap detector which is dominated by the overall reflection loss of the six photodiodes. The figure shows that the transmittance (solid squares) decreases from about 0.34 % at 400 nm to practically zero at 800 nm. The shown power responsivity was measured against a cryogenic radiometer using stabilized lasers.

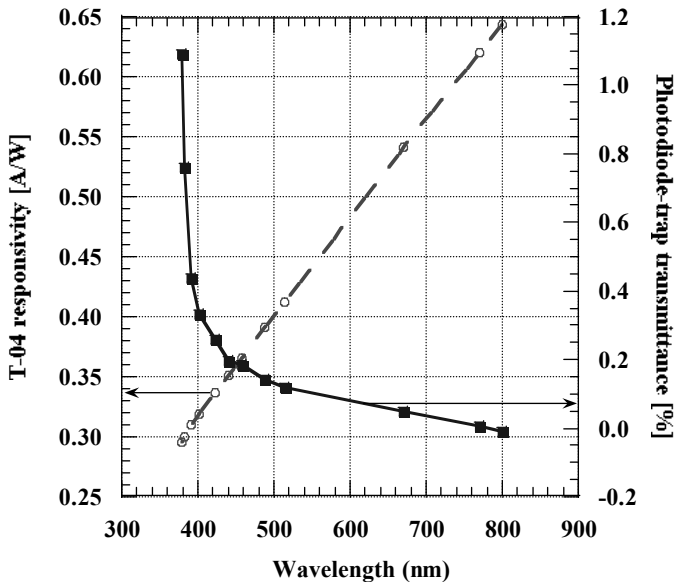


Fig. 1. Spectral power responsivity and transmittance of a Hamamatsu 1337 silicon photodiode-based tunnel-trap-detector.

<sup>1</sup> The mention of certain commercial products in this publication is for information purposes only and does not constitute an endorsement of the product by the author.

The external quantum efficiency (EQE) can be calculated from the IQE:

$$\text{EQE} = (1 - \rho)\text{IQE} \quad (2)$$

where  $\rho$  is the reflectance of the detector-surface. The equation shows that the surface reflectance loss is included in the external quantum efficiency. Surface coatings are often applied to reduce reflectance losses so that a device may more closely approach a maximum EQE in a given spectral range.

Figure 2 shows the EQE of two frequently used silicon photodiodes from Hamamatsu Corporation. Photodiode 1226 was developed for photometric (visible) applications therefore it has a suppressed EQE in the near-infrared range. The 1337 model was used to build the six-element tunnel-trap detector mentioned above. The figure shows that the EQE is much less than the unity (100 %) quantum efficiency, dominantly caused by the significant reflection loss.

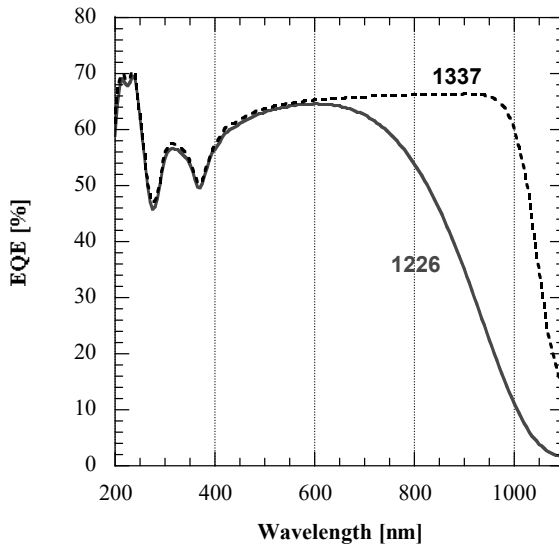


Fig. 2. EQE of two Hamamatsu fabricated single-element silicon photodiode models.

The spectral power responsivity is proportional to the EQE:

$$s(\lambda) = \text{EQE} \frac{e\lambda}{hc} = \text{EQE} * \lambda * \frac{1}{K} \quad (3)$$

where  $\lambda$  is the wavelength, and the proportionality factor  $1/K$  is calculated from three physical constants: the elementary electron charge  $e = 1.6021 * 10^{-19}$  Cb, the Planck's constant  $h = 6.6256 * 10^{-34}$  W/s<sup>2</sup>, and the velocity of light  $c = 2.997925 * 10^8$  m/s.

The spectral power responsivity and transmittance were measured at several laser lines to determine the IQE of the above discussed silicon tunnel-trap detector. The IQE is an important detector property which is determined by the detector fabrication technology. If it is close to unity, the detector reflectance-loss can be decreased with a trap design to obtain increased spectral responsivity for a given application. Figure 3 shows the EQE and the IQE of the above discussed (#04) tunnel-trap detector. The IQE was calculated from the EQE by replacing the measured trap-transmittance in place of the photodiode-reflectance in Eq. 2. The graph shows that the IQE is slightly higher than the EQE up to about 770 nm. The reflection loss (and the trap-transmittance) is negligibly small above 770 nm.

The EQE of three tunnel trap detectors is shown as a function of wavelength in Fig. 4. The trap-detectors were calibrated against a cryogenic radiometer using tunable lasers [2, 3]. The calibration (EQE determination) uncertainty was less than 0.1 % ( $k=2$ ). The three EQE functions are flat (constant) within +/- 0.15 % between 630 nm and 930 nm. According to this experimental verification, the silicon photodiode Model-1337 based tunnel-trap detectors can be used as intrinsic standards in this wavelength range. The mean EQE is 0.997 in this range with a relative standard uncertainty of 0.15 % ( $k=2$ ). Care should be made when this constant EQE is converted into responsivity, because the responsivity calculated from this EQE is wavelength dependent! The responsivity will be 0.5066 A/W at 630 nm (in good agreement with Fig.1) and 0.7479 A/W at 930 nm.

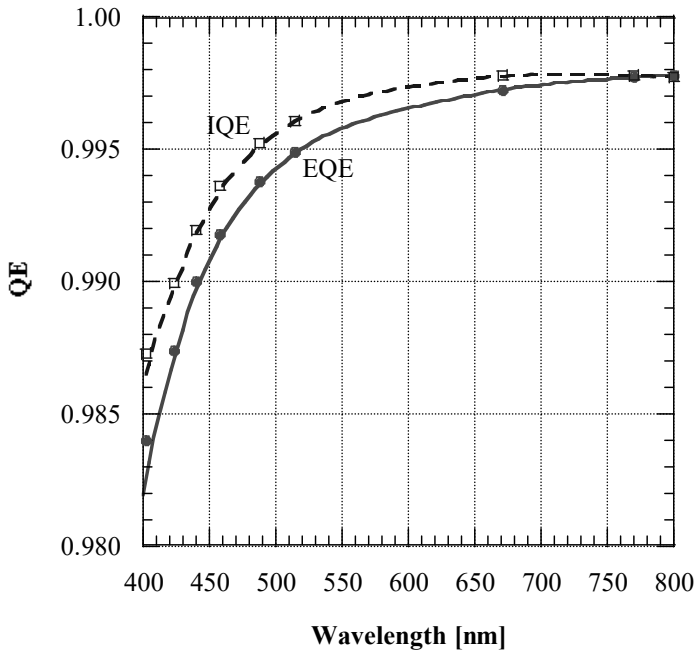


Fig. 3. The EQE and the IQE of a 1337 photodiode-based (#04) silicon tunnel-trap detector as calculated from the measured results shown in Fig. 1.

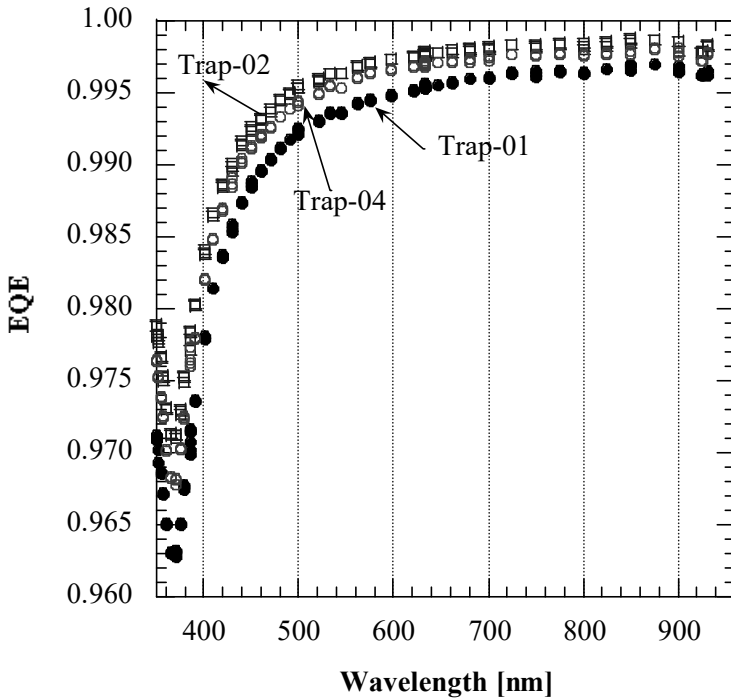


Fig. 4. EQE versus wavelength of three 1337 photodiode-based tunnel-trap detectors.

In addition to silicon photodiodes, single element GaP, GaAsP, PtSi, Nitrided Si, Ge, InGaAs, extended InGaAs, InSb, and photovoltaic (PV) HgCdTe (MCT) photodiodes can be utilized as standard- or test-detectors in the 200 nm to 5500 nm wavelength range. These photodiodes are made from different materials and have different energy-bands. Incident photons, with energy  $h\nu$  greater than the energy band gap, will create electron-hole pairs in the semiconductor at or near the junction. One of the most important radiometric characteristics of these detectors that propagate detector-based scales is spectral responsivity.

The spectral power responsivity of four single-element photodiodes that cover the 200 nm to 5500 nm wavelength range is shown in Fig. 5. The unity (100 %) quantum efficiency line is shown on the graph as well. The responsivity curves are always below the 100 %

quantum efficiency line because of the external reflection loss and internal losses that reduce the quantum efficiency. At the short-wavelength side, the responsivity functions are roughly parallel to the unity quantum efficiency line. This is dominantly caused by the roughly constant reflection loss versus wavelength that equally lowers the responsivity values relative to the unity quantum efficiency line at the short-wavelength sides.

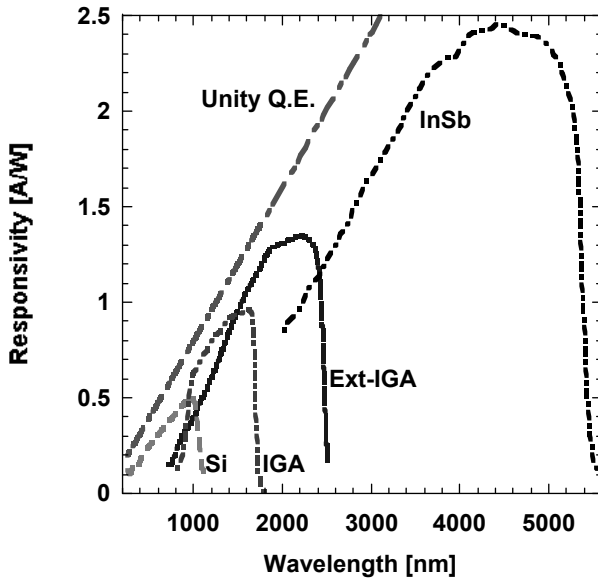


Fig. 5. Spectral responsivity of frequently used photodiodes for the 200 nm to 5.5  $\mu\text{m}$  range.

The Si curve shown in Fig. 5 is the spectral power responsivity of a Hamamatsu [4] Model 1337 photodiode. This photodiode is made by planar diffusion technology. The Model 2281 has a different case (with BNC output connector) and it is fabricated with the same technology. These Si photodiodes have very high and spatially uniform IQE and they are the most frequently used photodiodes for the realization and propagation of spectral responsivity functions. The Models 1226 and 1227 (shown in Fig. 2) are PNN<sup>+</sup> type silicon photodiodes with a thick N<sup>+</sup> layer that brings the N-N<sup>+</sup> boundary close to the depletion layer resulting in suppressed infrared responsivity. The 1226 and 1227 models are suitable for photometric and colour

measurements and also for very high sensitivity (low noise) applications. The extra thin P layers in both the 1227 and 1337 models produce high ultraviolet responsivity.

Actually, the 200 nm to 5500 nm wavelength range can be covered with three photodiodes: Si, extended-InGaAs, and InSb. In addition to these three photodiodes, the responsivity curve of a regular InGaAs photodiode is also shown in Fig. 5. Regular InGaAs photodiodes are popular since they can be operated at room temperature (like silicon photodiodes) without cooling. They can exhibit electronic and radiometric characteristics similar to silicon photodiodes when they are cooled to about  $-30\text{ }^{\circ}\text{C}$  to  $-40\text{ }^{\circ}\text{C}$  (depending on photodiode model and detector-area). This cooling can be made with 2-stage TE coolers using a regular heat sink (passive cooling) to remove the dissipated heat from the cooler.

Figure 6 compares the spectral power responsivity of two different InGaAs photodiodes. These InGaAs spectral responsivities were measured at room temperature. The largest difference in the responsivity functions of the two InGaAs photodiodes is at the short wavelength-end. The graph also shows the spectral power responsivity of a TE cooled Ge photodiode.

Since InGaAs photodiodes have better electronic and radiometric characteristics than Ge photodiodes [5], applications of Ge photodiodes are shrinking. The main disadvantage of Ge photodiodes is the significant temperature dependence (see below).

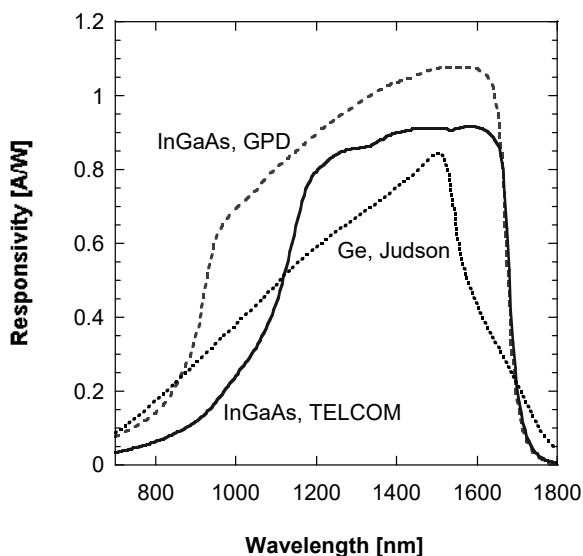


Fig. 6. Spectral power responsivity of a Ge and two different InGaAs photodiodes.

When using photodiodes at short wavelengths, care should be taken because ultraviolet (UV) damage can cause responsivity changes. Spectral responsivity curves of UV photodiodes are shown in Figs. 7 and 8. Figure 7 shows photodiodes that can be used for the UV-A wavelength range which is between 320 nm and 400 nm. UV damage caused changes can happen with GaP, GaAsP (not shown here), and regular Si photodiodes including the shown UV-100 photodiode. In order to avoid these changes, UV-damage resistant photodiodes, e.g. PtSi or nitride passivated Si detectors should be applied. For instance, the IRD fabricated UVG and AXUV Si photodiodes are both made with very thin, radiation-hard, junction passivating, oxynitride protective entrance window. This window makes them extremely stable even after exposure to intense UV radiation. The IRD AXUV-100G photodiodes are commercially available. They showed high stability even below 160 nm. Responsivity curves of photodiodes for the UV-B range are shown in Fig. 8. As shown, the responsivity of a PtSi Schottky photodiode is much lower than the responsivity of the other (shown) high-QE photodiodes. Also, they are rather noisy.

Care should be taken because the shown Si photodiodes are not solar-blind detectors. They also have responsivity outside of the UV to 1.1  $\mu\text{m}$ .

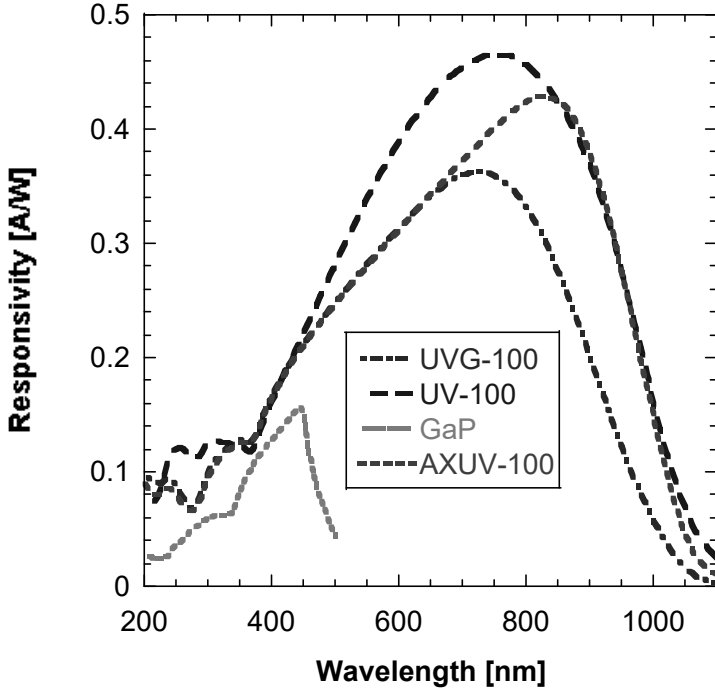


Fig. 7. Responsivity functions of UV photodiodes frequently used for the UV-A range.

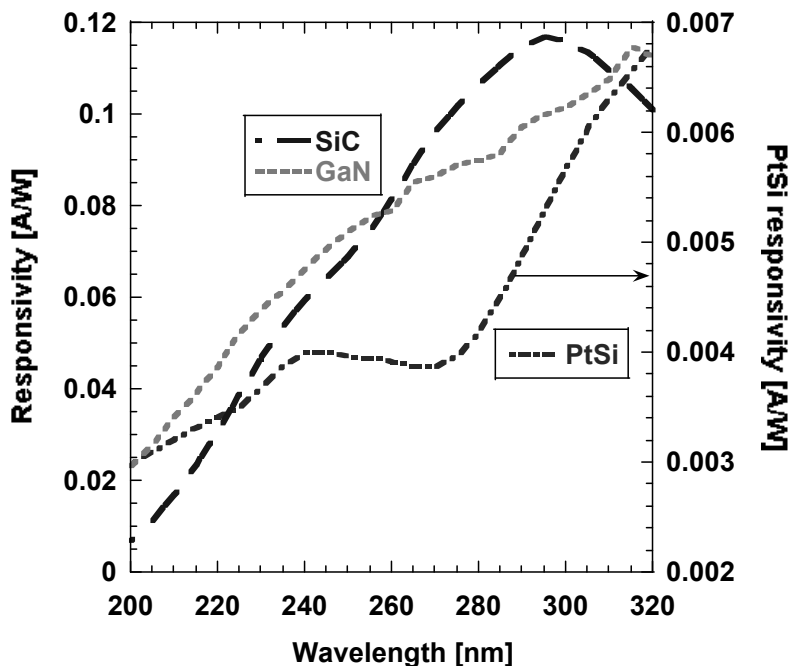


Fig. 8. Responsivity functions of UV photodiodes frequently used for the UV-B range.

The spectral responsivity variations of the model 1226 silicon photodiodes are illustrated in Fig. 9. The spectral power responsivity of four photodiodes were measured after taking them from the same batch. The largest maximum-to-minimum deviation of about 5 % can be seen at 800 nm.

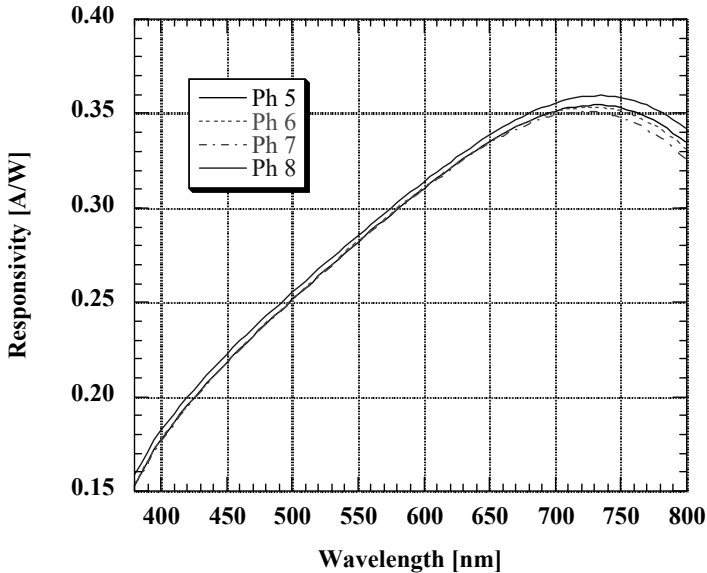


Fig. 9. Spectral responsivity variations of four silicon S1226-8BQ photodiodes from the same batch. The upper curve is Ph 8.

IR-enhanced Si photodiodes can be used as transfer standards. They can substitute Si trap detectors in an extended wavelength range between 300 nm and 1000 nm. Since the limitations of Si trap detectors (such as responsivity changes between 400 nm and 450 nm, increased spatial non-uniformity and temperature coefficient of responsivity above 950 nm) increase the sub 0.1 % ( $k=2$ ) responsivity uncertainties for wavelengths shorter than 350 nm and longer than 950 nm, this 5 mm diameter detector can be utilized in the overall 300 nm to 1000 nm range with an uncertainty of 0.1 % ( $k=2$ ). It is free of interference fringes and can be directly calibrated against a primary-standard cryogenic radiometer. After a 1-step scale transfer, the calibrated detector can be used as a reference detector for routine spectral responsivity calibrations of test detectors. It can measure both radiant power and irradiance with acceptance angles much larger than Si trap detectors. It has an  $NEP = 7 \text{ fW/Hz}^{1/2}$  which is more than a decade lower than that of a Si tunnel-trap detector. It does not need temperature control. The spectral power responsivity of this detector is shown in Fig. 10. The

peak of the spectral responsivity is at 1000 nm. The spatial and temperature dependent responsivities of this detector are discussed below in Sections 2.1.2 and 2.1.4.

Application of the shown Ext-IGA and InSb infrared photodiodes is more complicated than that of the UV to near-IR photodiodes. Typically, the Ext-IGA photodiodes need 4-stage TE cooling (to about  $-80\text{ }^{\circ}\text{C}$ ) to obtain good electronic and radiometric characteristics. Removing the dissipated heat from a 4-stage TE cooler needs either forced-air cooling or radiator-used water circulation. The InSb photodiodes operate in a cryogenic-Dewar at about liquid-nitrogen ( $77\text{ K}$ ) temperature.

Photovoltaic HgCdTe (PV MCT) detectors with  $2.8\text{ }\mu\text{m}$  cut-off wavelength have comparable characteristics to extended-InGaAs photodiodes. MCT detectors can be used in the  $2\text{ }\mu\text{m}$  to  $26\text{ }\mu\text{m}$  wavelength range (see Section 3.2 below). The maximum active size of a single-junction PV MCT photodiode is  $2\text{ mm}$ . Multiple-junction PV MCT detectors are commercially available with large ( $4\text{ x }4\text{ mm}$ ) active area. These detectors are cooled with 2-to-4 stage TE coolers and can cover the  $1.5\text{ }\mu\text{m}$  to  $12\text{ }\mu\text{m}$  wavelength range (see Volume-3: Optical Detector and Radiometer Standards).

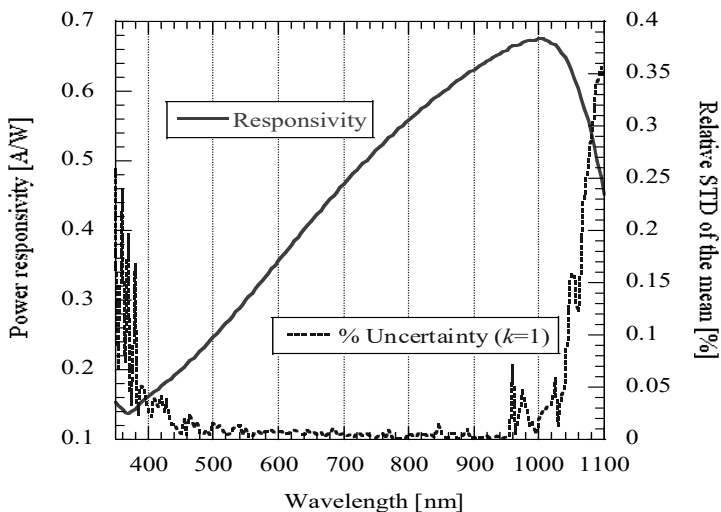


Fig. 10. Spectral power responsivity of an IR-enhanced Si photodiode, Hamamatsu Model S11499-01.

### 2.1.2. Spatial responsivity

Photodiodes have different sizes and their spatial non-uniformity of responsivity depends on photodiode types/models and material. In radiant power measurements where the photodiode active area is underfilled by the incident radiation to measure the total power in the incident beam, it is an important requirement from a photodiode to measure consistently (to get the same reading) at the different beam positions (inside of the active area of the photodiode) and within a given measurement uncertainty. When the position of the incident beam changes on the detector-surface, the spatial uniformity of responsivity must be known to estimate the responsivity changes and to determine the measurement uncertainty. Therefore, large area detectors with good spatial uniformity are needed for low-uncertainty radiant power measurements to avoid beam clipping and to measure the total power in the incident beam (focused on the detector).

In order to help selecting a photodiode for radiometric power measurement for a wide wavelength range with a required (low) power-measurement uncertainty, the non-uniformity of spatial responsivity of several large-area photodiodes (for radiometric applications) are shown below. The spatial non-uniformity of responsivity of the popular Hamamatsu 1337 silicon photodiode (which has a 10 mm x 10 mm active area) is shown in Fig. 11 at 500 nm. (Figs. 11 to 22, 28, 46, 47, and 48 are courtesy graphs from Thomas C. Larason of NIST.) The roughly 0.3 % maximum-to-minimum responsivity change remains similar to about 950 nm. At 1000 nm, the peak-to-peak spatial non-uniformity of responsivity increases to about 1 %. Therefore, Si trap detectors utilizing model 1337 (or 6337) photodiodes, should not be used for low-uncertainty measurements at wavelengths longer than 950 nm.

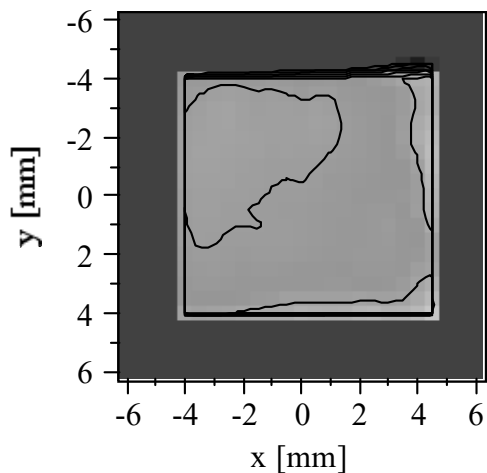


Fig. 11. Spatial non-uniformity of responsivity of a Hamamatsu Model 1337 Si photodiode at 500 nm. The contour lines show 0.2 % changes.

As shown in Fig. 12, an IR-enhanced Si photodiode (discussed above) has a maximum-to-minimum spatial non-uniformity of responsivity change of less than 0.2 % at 1000 nm. According to the measurement results shown in Fig. 13, the spatial non-uniformity of responsivity increases to 1 % level at 1050 nm.

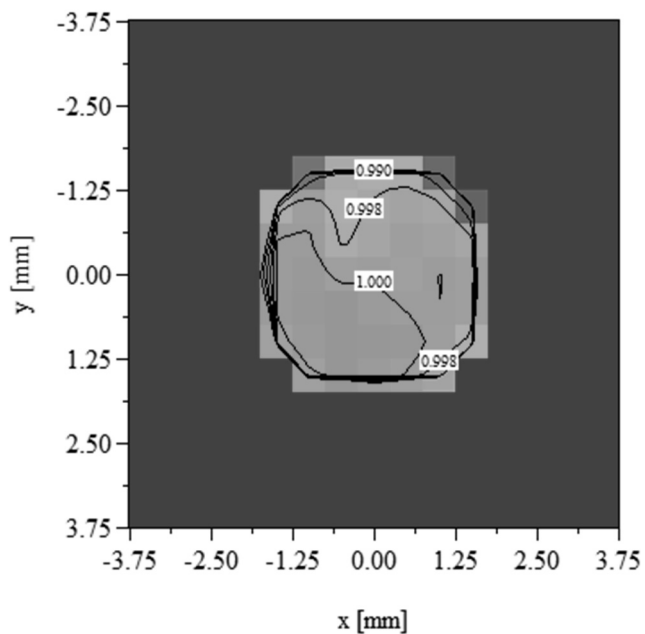


Fig. 12. Spatial non-uniformity of responsivity of an IR- enhanced Si photodiode, Hamamatsu Model S11499-01 at 1000 nm.

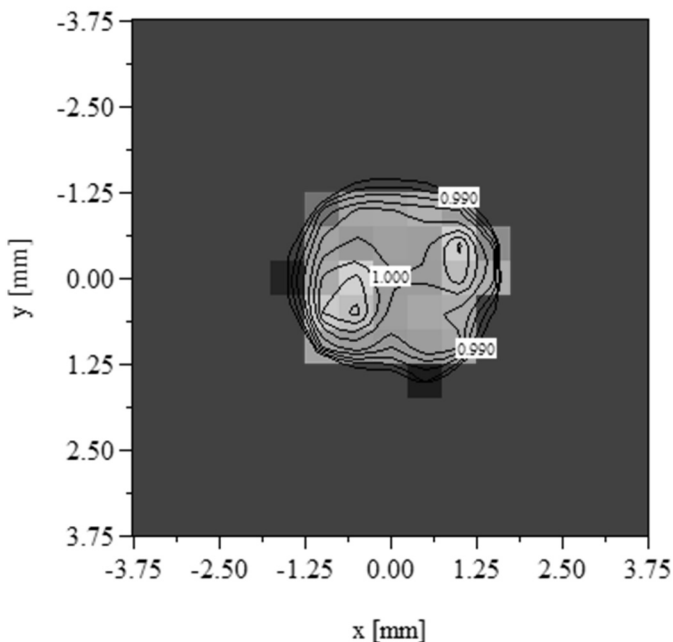


Fig. 13. Spatial non-uniformity of responsivity of an IR-enhanced Si photodiode, Hamamatsu Model S11499-01 at 1050 nm.

The non-uniformity of responsivity of a round silicon UV-100 photodiode, as shown in Fig. 14, is about 1.5 % (maximum-to-minimum) again at 500 nm. The non-uniformity of a GaP photodiode is shown in Fig. 15 at 340 nm. The contour lines were increased here from 0.2 % to 2 % to illustrate the 6 % to 8 % maximum-to-minimum responsivity changes over the active area. The 0.5 % contour-lines of a silicon AXUV-100G photodiode at 500 nm are shown in Fig. 16. The maximum-to-minimum responsivity change is about 0.5 %. Figure 17 shows that similar changes were measured on a PtSi photodiode at 300 nm. As shown in Fig. 18, the responsivity changes were similar on a UVG-100 photodiode at 300 nm. While Fig. 19 shows the non-uniformity of a Ge photodiode at 1500 nm, Fig. 20 shows the non-uniformity of a regular InGaAs photodiode at 1550 nm, 1650 nm, and 1750 nm. According to Fig. 20, the tested regular InGaAs photodiode has a roughly 1 % maximum-to-minimum responsivity change at 1650 nm. This change increases to about 3

% at 1750 nm which indicates that regular InGaAs photodiodes should not be used for low-uncertainty radiant power measurements at wavelengths longer than 1650 nm.

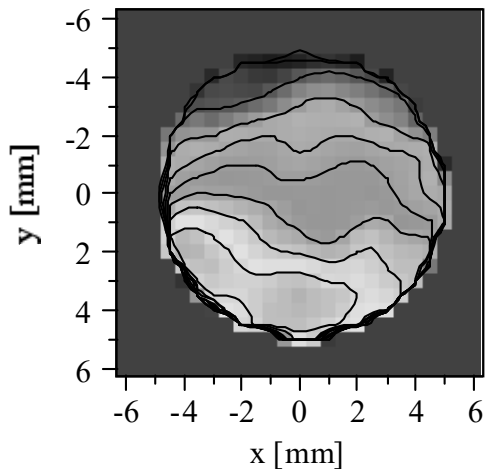


Fig. 14. The spatial non-uniformity of responsivity of a Si UV-100 photodiode is shown with 0.2 % contour-lines at 500 nm.

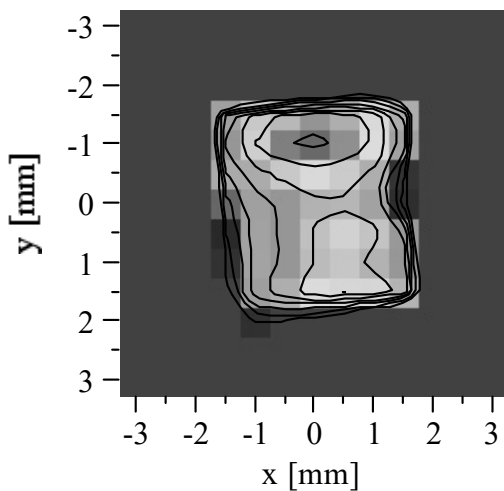


Fig. 15. The spatial non-uniformity of responsivity of a GaP photodiode is shown with 2 % contour-lines at 340 nm.